ЖЭТФ, 2012, том 142, вып. 6 (12), стр. 1212–1217

NEGATIVE DIFFERENTIAL CONDUCTANCE IN InAs WIRE BASED DOUBLE QUANTUM DOT INDUCED BY A CHARGED AFM TIP

A. A. Zhukov [a*], ***Ch. Volk*** [b,c], ***A. Winden*** [b,c], ***H. Hardtdegen*** [b,c], ***Th. Schäpers*** [b,c,d]

[a] *Institute of Solid State Physics, Russian Academy of Science*
142432, Chernogolovka, Russia

[b] *Peter Grünberg Institut (PGI-9), Forschungszentrum Jülich*
52425, Jülich, Germany

[c] *JARA-Fundamentals of Future Information Technology, Forschungszentrum Jülich*
52425, Jülich, Germany

[d] *II. Physikalisches Institut, RWTH Aachen University*
52056, Aachen, Germany

Received April 6, 2012

We investigate the conductance of an InAs nanowire in the nonlinear regime in the case of low electron density where the wire is split into quantum dots connected in series. The negative differential conductance in the wire is initiated by means of a charged atomic force microscope tip adjusting the transparency of the tunneling barrier between two adjoining quantum dots. We confirm that the negative differential conductance arises due to the resonant tunneling between these two adjoining quantum dots. The influence of the transparency of the blocking barriers and the relative position of energy states in the adjoining dots on the decrease in the negative differential conductance is investigated in detail.

Regarding the investigation of electronic transport of, one-dimensional systems such as InAs [1–5] and InN [6] nanowires, or carbon nanotubes [7, 8] became the focus of interest. One of the most effective methods to investigate such objects locally is a scanning gate measurement at room temperature [9] and helium temperatures [10, 11]. This technique was also used previously to investigate two-dimensional heterostructures [12–14] and graphene [15]. Furthermore, in scanning gate measurements performed at helium temperatures, the separation of an InAs nanowire in interconnected quantum dots of different sizes was demonstrated [10, 11].

Negative differential conductance (NDC) has been found in quantum dot structures of different types of realizations [16–20, 24]. It was observed in quantum dots defined by split gates on two-dimensional electron gases, where it has been regarded as a result of the presence of excited states weakly coupled to the main bath [16, 17]. A negative differential conductance has also been found in a linear array of metallic islands [18]. There, the NDC mechanism is based on the competition between the forward rate of injecting charges into a system, which increases with the bias, and the tunneling rate across some junctions, which can be reduced with increasing the bias [18]. A device consisting of a single electron transistor and an electron box attached to it as a gate was measured in [19]. The authors reported a negative differential conductance for a range of conditions. Furthermore, a negative differential conductance was observed in an especially grown InAs p–i–n light-emitting diode [20].

The aim of this paper is to induce a negative differential conductance in an InAs nanowire. Furthermore, we want to identify the mechanism of negative differential conductance in a sequentially connected double dot structure in a nanowire or nanotube (see [24]) by adjusting the thickness of the tunneling barrier between two adjoining quantum dots by a charged atomic force microscope (AFM) tip. In these experiments, a thick tunneling barrier is necessary to eliminate the strong increase in the current while the energy levels of the quantum dots are tuned out of resonance with increasing the source-to-drain voltage [25]. In Ref. [24], the electrochemical potential could only be changed in both dots simultaneously, whereas in our experiments, we

*E-mail: azhukov@issp.ac.ru

are able to shift the mutual positions of the energy states of both dots by means of a charged AFM tip. Therefore, our approach might help confirm the theoretical explanation suggested by Frannson and Eriksson [25]. The subject of our work is therefore to realize a negative differential conductance in an InAs wire by using a charged AFM tip and to investigate how this effect is influenced by the tunneling barrier thickness and the relative positions of energy levels of adjoining quantum dots.

The nominally undoped InAs nanowire used in our experiment was grown by selective-area metal–organic vapor-phase epitaxy [22]. The diameter of the wires is 100 nm. For the transport measurements, the nanowires are separated from the growth template and subsequently placed on a Si n-type doped (100) wafer covered with an SiO_2 insulating layer 100 nm thick. The doped silicon substrate is used as a back-gate to vary the electron density in the nanowire by applying a back-gate voltage V_{BG}. The evaporated ohmic Ti/Au contacts to the wires and the markers of the search pattern are defined by electron beam lithography and lift-off. For the sample studied here, the distance between the contacts is 3.5 μm. A scanning electron microscopy image of the sample under investigation is shown in Fig. 1 *a*.

All measurements are performed at $T = 4.2$ K. The charged tip of a home-built scanning probe microscope [23] for scanning gate imaging measurements is used as a relocatable gate. We keep the tip 300 nm above the SiO_2 surface to eliminate any mechanical or electrical contact of the tip to the nanowire. All scanning gate measurements are performed by keeping the potential of the scanning probe microscope tip (V_t) and V_{BG} constant. The electrical scheme of the scanning gate imaging measurements is shown in Fig. 1 *b*.

The conductance of the wire during the scan and the conductance as a function of the source-to-drain voltage (V_{SD}) and V_{BG} is measured in a two-probe scheme. A standard lock-in technique by applying a voltage and measuring the current with a current amplifier is used. The amplitude of the driving AC voltage is $V_{AC} = 0.1$ mV at a frequency of 231 Hz.

If $|V_t - V_{BG}| < 50$ meV, no influence of the tip on the conductance of the wire is observed for $V_{BG} > 5$V. At such high back-gate voltages, no dot in the wire is observed. Hence, the whole wire-to-back-gate capacitance is much lager than the wire-to-metallic-contacts ones and the potential of the wire is the same as V_{BG} in this case. The absence of the influence of the charged tip means that no additional impurity with its own charge is sited on the tip.

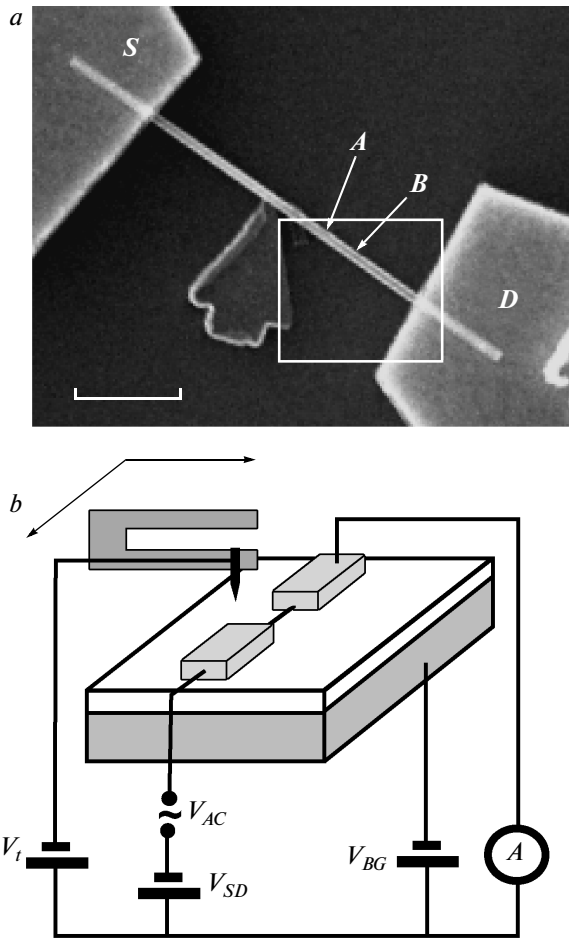

Fig. 1. *a*) Scanning electron microscope image of the InAs wire. Source and drain contact pads are marked by 'S' and 'D'. Positions of dots A and B are marked by arrows. The scale bar corresponds to 1 μm. The rectangle represents the area of scanning gate measurements at helium temperature. *b*) Electrical scheme of the measurements. The driving AC voltage is labeled as V_{AC}; the respective tip, gate, and source-to-drain DC voltages are labeled with V_t, V_{BG}, and V_{SD}

To localize the closed dot in our wire, a preliminary scanning gate measurement was performed (see Fig. 2 *a*). This scan was done at $V_{BG} = 1.725$ V, $V_{SD} = -8$ mV, and $V_t = 0$ V. The presence of two small dots in the wire is clearly visible. The centers of the dots are labeled by 'A' and 'B' in Fig. 2 *a*. Positions of the dots are defined from the shape of the equipotential line and the position of the wire itself. The accuracy of the definition of the dot positions is better than 100 nm and is comparable with the wire diameter. Both dots are formed by potential barriers created by defects of the wire crystal structure. Formation of dots of such a type was observed previously (see [10, 11]).

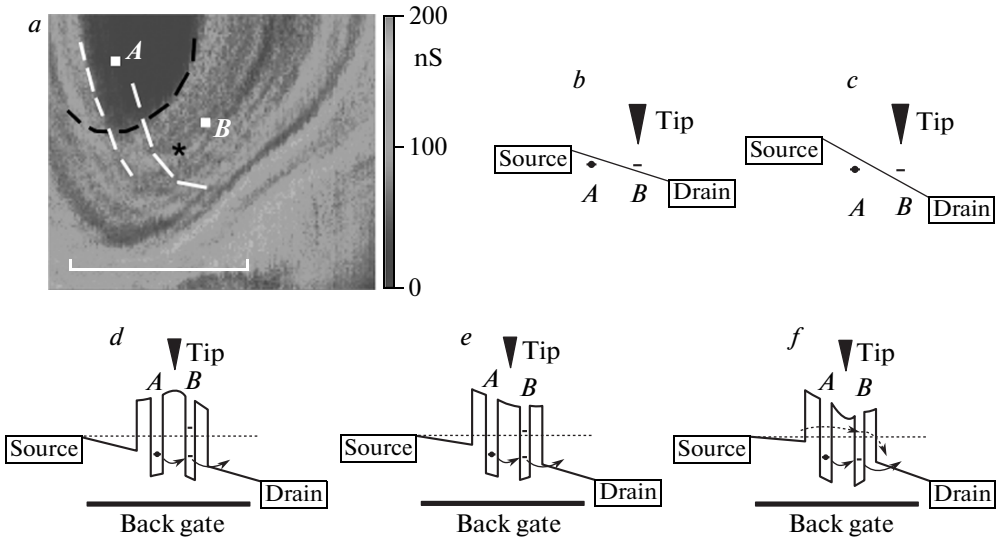

Fig. 2. *a*) Scanning gate measurement of the InAs wire made with $V_t = 0$, $V_{BG} = 1.725$ V, and $V_{SD} = 8$ mV. The position of the scanning area is marked with a square in Fig. 1*a*. The positions of the centers of dots A and B are marked by squares. The tip position during measurements of the conductance map as a function of V_{BG} and V_{SD} (see Fig. 3) is indicated by '$*$'. The dashed lines are guides to the eye and follow the equipotential lines of dot A (black) and B (white). The white horizontal bar corresponds to 1 μm. The side color bar represents the scale of the measured wire conductance. Figures *b*,*c* show the condition for the alignment of the energy levels of dots A and B for different tip voltages (V_t) and source-to-drain voltages (V_{SD}). To maintain the alignment of the energy levels of both dots, a higher source-to-drain voltage V_{SD} (Fig. *b*) $< V_{SD}$ (Fig. *c*) must be applied in the case where V_t (Fig. *b*) $> V_t$ (Fig. *c*) and where the distance from the tip to dot B is smaller than the corresponding distance to dot A. Images *d* to *f* demonstrate the modification of the band profile along the InAs wire with increasing V_t. An increase in V_t not only results in an increasing opacity of the drain-side blocking barrier (Fig. *e*) but also opens an additional conductivity channel through the energy state of dot B (Fig. *f*, dashed arrows)

No additional small and closed dots beyond dots A and B were observed with SGM scanning all over the wire.

For the next set of experiments, we placed the tip in an asymmetric position between the two dots but outside the wire to eliminate any possibility of mechanical or electrical contact between the charged tip and the dot (cf. the asterisk in Fig. 2*a*). By varying the tip voltage, we can simultaneously alter the opacity of depletion regions of the tunneling barrier separating the dots and change the mutual positions of the energy levels of the dots. The capacitance of the tip to the closer placed dot is larger than one of the tip to the dot at larger distance. The resulting wire conductance maps as functions of V_{SD} and V_{BG} measured at various tip voltages are presented in Fig. 3. A negative differential conductance is clearly visible in the experimental data measured at $V_t = 0$, 1 V, as can be seen in Fig. 3*a*,*b*. Remains of this effect are still observable in Fig. 3*c* ($V_t = 2$ V), while the negative differential conductance vanishes completely at $V_t = 3$ V, as can be seen in Fig. 3*d*. The inset of Fig. 3 shows the cross sections of Fig. 3*a*–*c* measured at $V_{BG} = 1.175$ V, 1.020 V, 0.910 V.

The experimental results of the scanning gate measurements are presented in Fig. 4. All measurements are performed at $V_t = 0$ and $V_{SD} = -8$ mV in accordance with the experimental data presented in Fig. 3 (inset). The V_{BG} values 1.1750 V, 1.1775 V, and 1.1800 V were applied during the respective scans in Fig. 4. The range of the back-gate voltages where an NDC is observed is in good agreement with the conductance mapping shown in Fig. 3*a*. Some asymmetry of the scanning gate imaging pictures is due to the nonperfect shape of the AFM tip.

We now discuss the obtained experimental results in more detail. It is easy to distinguish the double structure of the Coulomb diamonds dedicated to the two small closed quantum dots previously labeled as 'A' and 'B' (see Figs. 3*c*–*d*, dashed lines). This double structure is typical for quantum dots connected in series [11]. The negative differential conductance found at negative values of the V_{SD} has been observed previously in double-dot structures defined in a carbon nanotube [24] and has been explained in Ref. [25] by the asymmetry due to dots of different sizes.

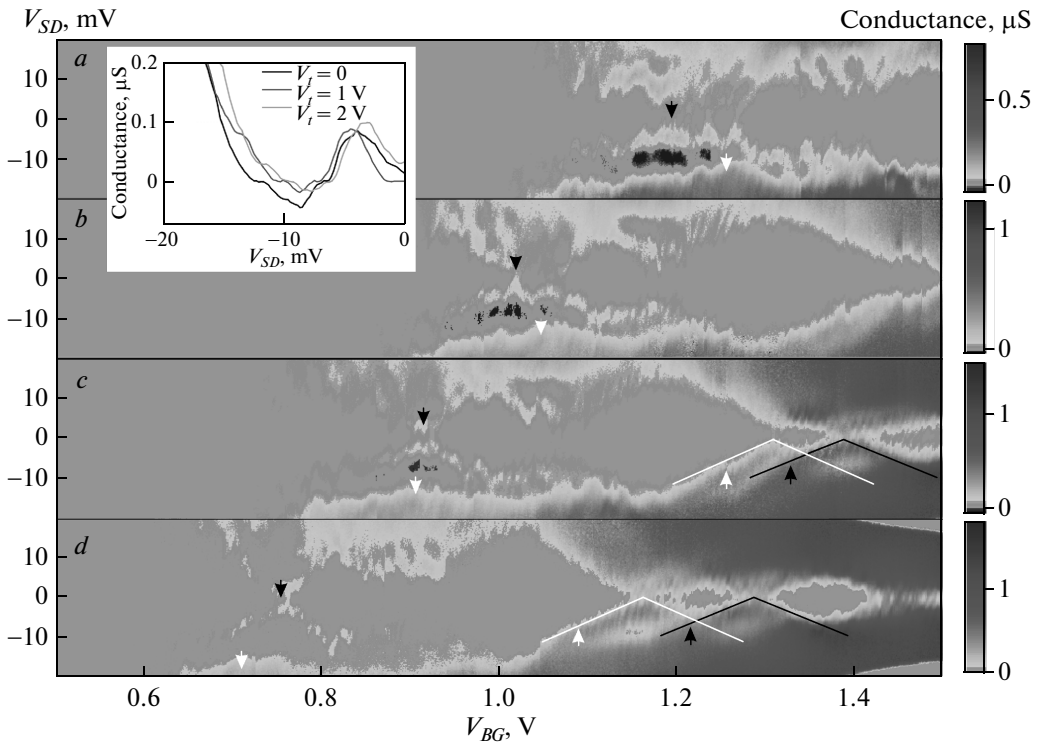

Fig. 3. *a–d*) Conductance maps of the InAs nanowire as a function of the source-to-drain voltage and back-gate voltage at different tip voltages $V_t = 0$, 1 V, 2 V, 3 V. The tip position is indicated in Fig. 2*d*. A negative differential conductance is clearly seen for measurements made at $V_t = 0$, 1 V. The arrows mark the conductance lines of Coulomb diamonds of dot A (black) and B (white) for high (noses up) and low (noses down) back-gate voltages. Lines on Figs. *c* and *d* are additional guides to the eye to emphasise the positions of the Coulomb diamonds of dot A (black) and dot B (white) for negative bias voltages. Note the mutual shift of the energy levels of dots A and B at different tip voltages. The inset shows cross sections of differential conductance vs. V_{SD} for different tip voltages $V_t = 0$, 1 V, 2 V respectively measured at $V_{BG} = 1.175$ V, 1.020 V, 0.910 V in (*a*), (*b*), and (*c*). The shift of the negative differential conductance to lower values of the V_{SD} for higher V_t is clearly visible. Artifacts in Fig. *d* at high biases and high V_{BG} are due to the overload of the current amplifier

The mutual positions of the energy levels of dots A and B strongly depend on the tip voltage and is governed by the different capacitance between the tip to dot A (c_{tA}) and the tip to dot B (c_{tB}) (see the arrow markers in Fig. 3). Comparing Figs. 3*c* and 3*d*, it is easy to see that position of Coulomb blockade diamond of dot A is shifted by 0.10 V (V_{BG} axis), while the diamond of dot B is shifted by 0.15 V when the tip voltage is increased by 1 V. The shift of the position Coulomb blockade diamond is proportional to $c_{tA(B)}/c_{A(B)-BG}$. Taking into account that $\alpha_A \approx \alpha_B = 0.1$ (where $\alpha_{A(B)} = c_{A(B)-BG}/c_{A(B)total}$, $c_{A(B)-BG}$ is the capacitance of dot A (B) to the back gate and $c_{A(B)total}$ is the total capacitance of dot A (B)) and the fact that parameter $\alpha_{A(B)}$ is strongly depended on the size of the dot formed with a wire or nanotube, we can conclude that $c_{A-BG} \approx c_{B-BG}$ and $c_{Atotal} \approx c_{Btotal}$. We hence obtain that $(c_{tB}/c_{B-BG})/(c_{tA}/c_{B-BG}) \approx c_{tB}/c_{tA} \approx 1.5$. This result is in good qualitative agreement with the geometry of the experiment (cf. Fig. 2*a*).

The relative position shift of the energy levels for dots A and B at different tip voltages results in a shift of the region where negative differential conductance occurs, as can be inferred from the experimental data in the inset of Fig. 3. This effect is also illustrated in Fig. 2*b*,*c*. To maintain the mutual energy level positions of the dots, the applied tip voltage in Fig. 2*b* must be larger than V_t in Fig. 2*c*.

In the set of experiments presented in Fig. 3, the increasing opacity of the tunneling barrier results in a suppression of the negative differential conductance, as can be seen in Fig. 2*d–f*. In Fig. 2*d*, the drain barrier of dot A is closed. The presence of a negative differential conductance is expected in this case when the energy level of dot A is shifted out of resonance with

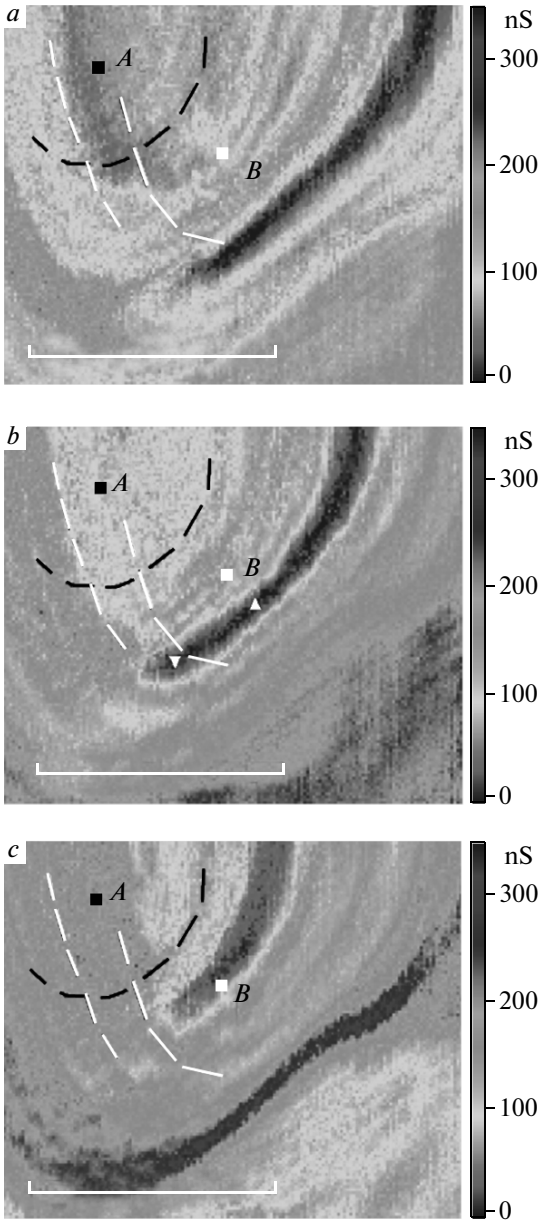

Fig. 4. Scanning gate measurements of an InAs wire measured at $V_t = 0$, $V_{SD} = 8$ mV, and $V_{BG} = 1.1750$ V (a), 1.1775 V (b), 1.1800 V (c) are presented. In Figs. b, and c, the negative differential line governed by the dot A conductance is eliminated abruptly while crossing the line of peak conductance of dot B. The scale bar corresponds to 1 μm for all three images. The white triangles mark positions of the tip used to evaluate the mutual shift of the energy levels of quantum dots

the lower energy level of dot B. In Fig. 2e, the barrier is slightly open, whereas in Fig. 2f, the barrier is open completely with the consequence that the negative differential conductance is destroyed. This is in agreement with theoretical calculations made by Fransson and Eriksson [25].

In case of narrow energy level widths for both dots, the NDC must be present in scanning gate measurements as one or two small areas placed symmetrically against the wire axis. According to the inset of Fig. 3, the NDC is quite stable with respect to mutual energy level positions of both dots and therefore the area of NDC in scanning gate measurement looks like a line, as can be seen in Fig. 4a,b.

An additional mechanism of the negative differential conductance suppression is also presented in the set of scanning gate measurements. Figure 4b demonstrates the decrease of the negative differential conductance effect when the line of negative differential conductance of dot A crosses the conductance peak line of dot B. A similar but less pronounced effect is observed in Fig. 4a. Thus, by using the scanning gate measurements, we found that the additional conductivity channel through the higher energy state of dot B plays a crucial role in suppressing of the negative differential conductance as the tip moves along the equipotential line of dot A. This mechanism is depicted in Fig. 2f, where the additional channel through the upper energy level of dot B is labeled by a dashed arrow.

To show that negative differential conductance is not suppressed by the shift of the mutual energy level positions of the dots, we calculate this shift in the case where the tip is moving along an equipotential line from the tip closest to the dot B position (marked with up nose white triangle, Fig. 4b) to the most distant position where the negative differential conductance is observed (marked with down nose white triangle, Fig. 4b). We use the bottom part of the picture because the upper part is deformed by a nonperfect shape of the tip. Taking into account that the center of the tip is placed approximately $\Delta z = 400$ nm above the sample surface, it is possible to represent the dependence of the tip-to-dot capacitance on the lateral distance between the center of the dot A (B) and the tip position ($\Delta r_{A(B)}$) as $c_{tA(B)} \propto f_c(r_{A(B)}) = (\Delta r_{A(B)}^2 + \Delta z^2)^{-0.5}$. This approximation works quite well because the calculated value $f_c(r_{B1})/f_c(r_{A1}) = c_{tB}/c_{tA} = 1.52$ is in good agreement with the experimentally obtained value 1.5; here, $r_{A1} = 0.25\mu$m and $r_{B1} = 0.6\mu$m are the lateral distances from the tip to dot A and dot B (see Fig. 2a). Using this approximation it is therefore possible to evaluate the mutual shift of the energy levels $\Delta_{Emutual} =$

$= \alpha\alpha_t\Delta V(f_c(r_{Bcl}) - f_c(r_{Bfar}))/f_c(r_{B1}) = 3.3$ meV, where $\alpha = c_{B-BG}/c_{Btotal} = 0.1$, $\alpha_c = c_{tB}/c_{B-BG} = 0.1$, $\Delta V = V_{BG} - V_t = 1.2$ V (these are the voltages in scanning gate microscopy measurements presented in Fig. 4), and $r_{Bcl} = 0.2\mu$m and $r_{Bfar} = 0.45\mu$m are the closest and the farthest lateral distances from the tip to the center of dot B (see Fig. 4*b*). The obtained value is less than 5 meV of the experimentally observed negative differential conductance region for $V_t = 0$ (see the inset to Fig. 3). The mutual shift of the dot energy levels calculated for Fig. 4a is equal to 2.0 meV.

When the tip is placed above one of the dots (dot B) while the negative differential conductance takes place (see Fig. 3*c*), the mechanism of the negative differential conductance decrease is not quite clear. The energy level misalignment of both dots and the increasing opacity of the tunneling barrier between them occur simultaneously, and it is therefore impossible to distinguish between these mechanisms of destruction.

In conclusion, we performed transport measurements at helium temperatures on a back-gated InAs nanowire at low electron density when the wire is split into quantum dots connected in series. By adjusting the opacity of the tunneling barrier between the two closed quantum dots by means of a charged AFM tip, a negative differential conductance is induced in the system. The shift of the V_{SD} regions where the NDC occurs while a different tip voltage induces an alteration of the mutual energy level positions of the dots confirms the explanation suggested in Ref. [25]. It is shown that a suppression of the negative differential conductance can be attributed to an additional conductivity channel through the energy state of the neighboring quantum dot if the tip also moves along a particular equipotential trajectory.

This work was supported by the Russian Foundation for Basic Research (grants №№ 10-02-00198-a, 11-02-00620-a, 11-02-12071-ofi-m-2011, 12-02-00272-a), and by the International Bureau of the German Federal Ministry of Education and Research within the project RUS 09/052.

REFERENCES

1. A. C. Ford, J. C. Ho, Yu-Lun Chueh et al., Nano Lett. **9**, 360 (2009).
2. C. Thelander, T. Martensson, M. T. Björk et al., Appl. Phys. Lett. **83**, 2052 (2003).
3. M. Scheffler, S. Nadj-Perge, L. P. Kouwenhoven et al., J. Appl. Phys. **106**, 124303 (2009).
4. C. Blömers, M. I. Lepsa, M. Luysberg et al., Nano Lett. **11**, 3550 (2011).
5. S. Wirths, K. Weis, A. Winden et al., J. Appl. Phys. **110**, 053709 (2011).
6. Th. Richter, Ch. Blömers, H. Lüth et al., Nano Lett. **8**, 2834 (2008).
7. A. Makarovski, A. Zhukov, J. Liu, and G. Finkelstein, Phys. Rev. B **76**, 161405(R) (2007).
8. A. Makarovski, A. Zhukov, J. Liu, and G. Finkelstein, Phys. Rev. B **75**, 241407(R) (2007).
9. A. A. Zhukov, Ch. Volk, A. Winden, H. Hardtdegen, and Th. Schäpers, Physica E **44**, 690 (2011).
10. A. C. Bleszynski, F. A. Zwanenburg, R. M. Westervelt et al., Nano Lett. **7**, 2559 (2005).
11. A. A. Zhukov, Ch. Volk, A. Winden, H. Hardtdegen, and Th. Schäpers, JETP Lett. **93**, 13 (2011).
12. R. Crook, C. G. Smith, A. C. Graham et al., Phys. Rev. Lett. **91**, 246803 (2003).
13. A. Pioda, S. Kicin, T. Ihn et al., Phys. Rev. Lett. **93**, 216801 (2004).
14. P. Fallahi, A. C. Bleszynski, R. M. Westervelt et al., Nano Lett. **5**, 223 (2005).
15. S. Schnez, J. Güttinger, M. Huefner et al., Phys. Rev. B **82**, 165445 (2010).
16. A. T. Johnson, L. P. Kouwenhowen, W. de Jong et al., Phys. Rev. Lett. **69**, 1592 (1992).
17. J. Weis, R. J. Haug, K. V. Klitzing, and K. Ploog, Phys. Rev. Lett. **71**, 4019 (1993).
18. H. Nakashima and K. Uozumi, J. Appl. Phys. Jpn. **34**, L1659 (1995); H. Nakashima and K. Uozumi, J. Vac. Sci. Technol. B **15**, 1411 (1997).
19. C. P. Heij, D. C. Dixon, P. Hadley, and J. E. Mooij, Appl. Phys. Lett. **74**, 1042 (1999).
20. A. Krieg and X. L. Huang, Appl. Phys. Lett. **86**, 061113 (2005).
21. F. Capasso, S. Sen, and A. C. Gossard, IEEE Electr. Dev. Lett. EDL-7, 573 (1986).
22. M. Akabori, K. Sladek, H. Hardtdegen, Th. Schäpers, and D. Grützmacher, J. Cryst. Growth **311**, 3813 (2009).
23. A. A. Zhukov, Instr. Exp. Tech. **51**, 130 (2008).
24. K. Ishibashi, M. Suzuki, T. Ida, and Y. Aoyagi, Appl. Phys. Lett. **79**, 1864 (2001).
25. J. Fransson and O. Eriksson, Phys. Rev. B **70**, 085301 (2004).